Research Square

Preprints are preliminary reports that have not undergone peer review.
They should not be considered conclusive, used to inform clinical practice,
or referenced by the media as validated information.

Regulation of brain iron uptake by apo- and holo-transferrin is dependent on sex and delivery protein

Stephanie L. Baringer
Penn State College of Medicine
Elizabeth B. Neely
Penn State College of Medicine
Kondaiah Palsa
Penn State College of Medicine
Ian A. Simpson
Penn State College of Medicine
James R. Connor (jrc3@psu.edu)
Penn State College of Medicine

Research Article

Keywords: Blood-brain barrier, iron, H-ferritin, transferrin, sex difference

Posted Date: March 16th, 2022

DOI: https://doi.org/10.21203/rs.3.rs-1443502/v1

License: This work is licensed under a Creative Commons Attribution 4.0 International License.
Read Full License

Abstract

Background: The brain requires iron for a number of processes, including energy production. Inadequate or excessive amounts of iron can be detrimental and lead to a number of neurological disorders. As such, regulation of brain iron uptake is required for proper functioning. Understanding both the movement of iron into the brain and how this process is regulated is crucial to both address dysfunctions with brain iron uptake in disease and successfully use the transferrin receptor uptake system for drug delivery.

Methods: Using *in vivo* steady state infusions of apo- and holo-transferrin into the lateral ventricle, we demonstrate the regulatory effects of brain apo- and holo-transferrin ratios on the delivery of radioactive ^{55}Fe bound to transferrin or H-ferritin in male and female mice. In discovering sex differences in the response to apo and holo Tf infusions, ovariectomies were performed on female mice to interrogate the influence of circulating estrogen on regulation of iron uptake.

Results: Our model reveals that both sex and type of iron delivery protein have significant effects on the regulation of iron uptake into the microvasculature and subsequent release into the brain. Furthermore, we show that cells of the microvasculature act as significant reservoirs of iron and release the iron in response to cues from the interstitial fluid of the brain.

Conclusions: These findings extend our previous work to demonstrate that the regulation of brain iron uptake is influenced by both the mode in which iron is delivered and sex. These findings further emphasize the role of the microvasculature in regulating brain iron uptake and the importance of cues regarding iron status in the extracellular fluid.

Background

Iron plays an essential role in many important biological functions, including cognition and overall brain health. As an electron donor and acceptor, as well as a carrier of oxygen, iron is vital to cellular metabolism[1]. Furthermore, iron is utilized in both the formation of myelin and the synthesis of many neurotransmitters, such as dopamine and norepinephrine[1]. Fluctuation of optimal iron levels can cause many neurological issues. Low levels of brain iron in adults are connected to Restless Legs Syndrome[2,3] and sleep disorders[4]. On the other hand, excessive brain iron is linked to many neurodegenerative disorders[5], such as Parkinson's disease[6], amyotrophic lateral sclerosis[7], and Alzheimer's disease[8,9]. The importance of iron homeostasis for neurological health and proper functioning requires tight regulation at the blood-brain barrier (BBB).

Previously it was posited that endothelial cells (ECs) of the BBB, which make up approximately 2% of the brain[10], passively transport iron from blood to brain. The premise was that holo-transferrin (Tf) (iron rich) bound to its receptor, on the luminal membrane and was transcytosed to the abluminal space. However, this model did not consider the iron needs of the ECs nor did it acknowledge the clear need for regulation of iron access to the brain. Our laboratory and others have since demonstrated regulation of iron uptake

by ECs[11–16]. Specifically, our group has shown that apo-Tf (iron poor) in the basal space increases both iron transport and release from ECs *in vitro*[14]. Furthermore, the Tf transcytosis theory does not account for the delivery of iron to the brain by H-ferritin (Fth1), which has gained increasing interest as an iron delivery protein[17–19]. In addition to our group's previous work exploring the *in vitro* effects of apo- and holo-Tf, Chiou *et al.* have suggested that iron uptake into the brain is regulated by ECs, which control uptake into the cells, storage of iron therein, and subsequent release into the brain[14]. In the present study we examined both the uptake of iron within the microvasculature and its subsequent release into the brain parenchyma. Moreover, we hypothesized that sex differences, which have been shown to be prominent in brain iron acquisition[18,20,21], would be subject to regulation of iron uptake by apo- and holo-Tf as well as the type of iron delivery protein.

Methods

Experimental Design

Mini osmotic pumps were inserted subcutaneously connected to a cannula inserted in the lateral ventricle (Fig. 1). After 48 hours of infusion, animals were injected intraperitoneally with either ^{55}Fe-Tf or ^{55}Fe-Fth1. Twenty-four hours later, brains were harvested and separated into microvessel and whole brain fractions. The tissue was then solubilized and counted using liquid scintillation counting.

Pump Surgery

Forty-eight hours prior to the surgery, osmotic pumps (Alzet, model 2004) were filled according to manufacturer instructions with nothing (sham), artificial cerebrospinal fluid (aCSF, 125 mM NaCl, 2.5 mM KCl, 1 mM MgCl-6H_2O, 1.25 mM NaH_2PO_4, 2 Mm CaCl-2H_2O, 25 Mm $NaHCO_3$, 25 mM glucose, pH 7.3), 1 mg/ml apo-Tf in aCSF, or 1 mg/ml holo-Tf in aCSF. Three-month-old wildtype (B6;129X1-Hfetm1Jrco/J background) mice were subjected to pump insertion under isoflurane anesthesia (1%-2%). A power analysis revealed n = 5 was required for 80% at alpha 0.05. Briefly, the pump with attached tubing was placed subcutaneously and the cannula was placed 1 mm lateral to Bregma and 0.5 mm posterior to deliver the pump contents directly to the lateral ventricle. This placement was considered sufficient to influence iron uptake by the microvasculature given that the well-established dynamic equilibrium of CSF and interstitial fluid, allowing the pump contents to distribute throughout the brain parenchyma[22]; similar to endogenous Tf produced by the choroid plexus[23]. The inclusion of aCSF as an experimental condition allows us to exclude the vehicle to be the cause of changes and informs us of general infusion effects and to determine any dilution effect of the endogenous Tf on the iron uptake. The incision was then sutured with nylon sutures. The mice were then placed in a heated recovery chamber until they regained consciousness, and accordingly, they were returned to their cages. Mice were maintained under normal housing conditions. They were given ad libitum access to rodent chow pellets and water. Both males and females were included in experiments. This study complies with the ARRIVE 2.0 guidelines. All procedures were conducted according to the NIH Guide for the Care and Use of Laboratory Animals and were

approved by the Pennsylvania State University College of Medicine Institutional Animal Care and Use Committee.

Iron Protein Preparation

Wild-type human Fth1 containing a poly-His tag was subcloned into pET30a(+), to be produced in BL21 *Escherichia coli*[17]. Isopropyl-β-D-thio-galactoside (IPTG) was used to induce expression. Following this, bacteria were lysed, and Fth1 protein was purified on a nickel column using standard techniques (GE Healthcare Bio-Sciences). Transferrin was purchased commercially (Sigma).

Radiolabeling

^{55}Fe (Perkin Elmer) was complexed with 1 mM nitrilotriacetic acid (NTA), 6 mM ferric chloride ($FeCl_3$), and 0.5 M sodium bicarbonate ($NaHCO_3$) at a ratio of 100µL NTA: 6.7µL $FeCl_3$: 23.3µL $NaHCO_3$: 50µCi $^{55}FeCl_3$ to form the ^{55}Fe-NTA complex[14]. After complexing, ^{55}Fe-NTA was incubated with apo-Tf (Sigma) or Fth1 for 30 minutes to allow for iron loading. Unbound iron was separated from the total complex using PD midiTrap-G25 columns following manufacturer's instructions (GE Healthcare Bio-Sciences).

Uptake Studies

Mice received a single intraperitoneal injection of 3.4 mg/kg body weight ^{55}Fe-Tf or ^{55}Fe-Fth1. 24 hours after injection, blood was drawn and mice were transcardially perfused with 0.1M phosphate-buffered saline (PBS, pH 7.4). Brains were collected, weighed immediately, and homogenized on ice using disposable tissue grinders (VWR) and MVB Buffer (0.147 M NaCl, 0.4 mM KCl, 0.3 mM CaCl2, 0.12 mM MgCL2, 15 mM HEPES, 0.5% BSA, 5 mM glucose). Homogenates were transferred to microcentrifuge tubes and spun at 1000 x g for 10 minutes at 4°C. The supernatant was collected, and the pellet was resuspended in buffer and spun again. The resulting supernatant was combined with the previous collection and termed whole brain. The pellet was resuspended again and termed microvessels (MVs). Validation of these fractions can be found in Fig. 1. This separation allowed us to determine the amount of ^{55}Fe that entered the brain or was sequestered in the MVs. Tissue was solubilized using 1 mL Solvable (Perkin Elmer) according to manufacturer's instructions. After solubilization, 10 mL Hionic-Fluor scintillation cocktail (Perkin Elmer) was added. Samples were counted using the Hidex 300 SL (LabLogic) for three minutes each. Blank tube values were subtracted from final counts to correct for background counts.

Protein Detection

Brain homogenates were spun at 1000 x g for 10 minutes at 4°C[20]. The supernatant (cortical fraction) was spun at 14000 x g for 10 minutes. The resulting cell pellet was resuspended and digested in RIPA buffer (Sigma) containing protease inhibitor cocktail (PIC, Sigma) for 1 hour on ice. The MV pellet was resuspended and digested in a mixture of RIPA buffer (Sigma) and protease inhibitor cocktail (PIC, Sigma) for 1 hour on ice. All homogenates were sonicated on ice for 90 seconds and spun at 14000 x g for 10 minutes at 4°C for final collect of the protein lysate. Total protein was quantified by bicinchoninic

assay (BCA, Pierce) and 25 µg was loaded onto a 4–20% Criterion TGX Precast Protein Gel (Bio-Rad). Protein was transferred onto a nitrocellulose membrane and probed for the neuronal marker TUJ1 (Abcam, 1:1000, ab18207) or the brain MV marker von Willebrand factor (Abcam, ab174290, 1:1000) and cyclophilin B as a loading control (Abcam, ab16045, 1:1000). Corresponding secondary antibody conjugated to HRP was used (1:5000, GE Amersham) and bands were visualized using ECL reagents (Perkin-Elmer) on an Amersham Imager 600 (GE Amersham).

Ovariectomy

Two-month-old female mice were subjected to aseptic bilateral surgical ovariectomy (OVX) via a dorsal incision under isoflurane anesthesia (1%-2%). After surgery, the skin was sutured with nylon sutures. These mice were then placed in a heated recovery chamber until they regained consciousness, and accordingly, they were returned to their cages. After two weeks, blood was collected from OVX mice and four equally aged intact mice to act as a control.

Serum Molecule Detection

Blood was collected via submandibular cheek blood collection in heparin-coated tubes. Serum was separated from whole blood fractions by centrifugation at 2000 x g for 15 minutes. Serum levels of estradiol were measured by enzyme-linked immunosorbent assay (Cayman Chemical, 501890) according to the manufacturer's protocol. Total iron binding capacity (TIBC), transferrin percent saturation, and serum iron were measured using an assay kit (Abcam, ab239715).

Statistical Analysis

Statistical analyses were performed using Prism 9.2 software (Graphpad Software Inc.). Data from at least five independent biological replicates were averaged and are expressed as the mean ± standard deviation (SD). One-way ANOVA with Tukey post-hoc analysis or unpaired t-tests were used to evaluate for statistical significance where appropriate. A p-value < 0.05 was considered significant.

Results

^{55}Fe-Tf uptake is responsive to apo- and holo-Tf in a sex-dependent manner

The aim of the first study was to examine the regulatory effects of apo- and holo-Tf on ^{55}Fe-Tf uptake. In males, both ^{55}Fe-Tf uptake (Fig. 2a) and release (Fig. 2b) were significantly increased with apo-Tf infusions ($*p < 0.05$) by nearly 41%. In contrast, infusion of holo-Tf resulted in levels of ^{55}Fe-Tf uptake and release significantly lower than observed with apo-Tf infusion ($*p < 0.05$ and $**p < 0.01$). The infusion of aCSF increased ^{55}Fe-Tf uptake and release, though not statistically significant or to the same level as apo-Tf. However, in females, ^{55}Fe-Tf uptake into MVs (Fig. 2c) and release into the brain (Fig. 2d) were unaltered in response to apo- and holo-Tf infusions. Notably, about 50% more ^{55}Fe-Tf was sequestered in the MVs than was released into the brain, supporting the regulator role of the MVs regardless of sex.

^{55}Fe-Fth1 uptake is not responsive to apo- or holo-Tf

The regulation of ^{55}Fe-Fth1 uptake and release by apo- and holo-Tf infusion was examined next. In male mice, ^{55}Fe-Fth1 uptake into MVs (Fig. 3a) and release into the brain (Fig. 3b) was not significantly different in response to either holo or apo Tf infusion. Similarly, in female mice, ^{55}Fe-Fth1 uptake into MVs was unaltered with the respective infusions (Fig. 3c), however, release into the brain (Fig. 3d) increased with infusion of apo-Tf by about 43% compared to sham but with considerable variability. Thus, the results were not statistically significant. As was the case with Tf delivered iron, uptake of Fth1 into the MVs was 50% higher than that released into the brain for both sexes.

Iron uptake is strongly carrier protein- and sex-dependent

Next, baseline differences in total iron uptake between sexes and carrier proteins were established by pooling the ^{55}Fe uptake into the MVs and release into the whole brain (Fig. 4a) from the sham control group. Males had little difference in total ^{55}Fe uptake whether bound to Tf or Fth1, whereas females took up 55% more iron when bound to Tf compared to Fth1 (*$p < 0.05$). On completing this analysis, it became apparent that there was a noticeable difference in variability of ^{55}Fe-Tf total uptake between males and females. Therefore, the coefficient of variation, which is the ratio of the standard deviation to the mean, was determined for ^{55}Fe-Tf uptake in sham groups in both sexes. The coefficient of variation was 17.43% in males and 45.09% in females. This level of variance in females suggested the existence of a confounding variable. The proportion of ^{55}Fe released into the whole brain to the ^{55}Fe taken up by the MVs was also compared between the sexes. In females, compared to males, the proportion of ^{55}Fe-Tf released to ^{55}Fe-Tf taken up into the MVs was significantly higher (Fig. 4b, *$p < 0.05$). When bound to Fth1, the proportion of ^{55}Fe released was not different between males and females (Fig. 4c).

Reduction of circulating estrogen does not impact ^{55}Fe-Tf uptake regulation

To determine whether the variation within the female dataset was related to the estrus cycle, circulating estrogen was removed by performed ovariectomies (OVX) on 2-month-old female mice. We hypothesized that removal of estrogen would reduce variability and result in female ^{55}Fe-Tf uptake and regulatory pattern similarly to the males. Two weeks after the OVX surgery, serum was isolated from the blood of the mice and confirmed their reduced estradiol levels (Fig. 5c). Three-month-old OVX mice displayed ^{55}Fe-Tf uptake by MVs (Fig. 4a) and release into the brain (Fig. 4b) that was unaltered by any infusion compared to sham, as observed in the intact female mice. However, the coefficient of variation of the total ^{55}Fe uptake in sham conditions was 16.15% for the OVX group, which was more comparable to male variance (17.43%) than intact females (45.09%). In order to better understand the systemic iron status of the OVX mice, we further analyzed the serum isolated from the mice by examining the total iron binding capacity (TIBC) and serum iron levels (Fig. 5d). TIBC was higher in OVX mice (427.5 μmol/L) compared to intact control mice (341.2 μmol/L). Serum iron was lower in OVX mice (90.6 μmol/L) compared to the control

(110.0 µmol/L). Lastly, Tf saturation percentage was decreased in OVX (23.0%) compared to control (32.4%). These measures indicate reduced systemic iron levels, but not enough to be deemed iron deficient.

Conclusions

The objective of this study was to determine the regulation of Fth1- and Tf-bound iron uptake into the brain by apo- and holo-Tf *in vivo.* In pursuit of this aim, we discovered significant sex differences in the regulation of iron uptake mediated by these two proteins. The results of this study have demonstrated that the ratio of apo- to holo-Tf in the CSF regulates Tf-bound iron uptake in males, but not in females in this model. However, there was significant variation in ^{55}Fe-Tf uptake in females. To address these differences, we performed ovariectomies aimed to determine if reducing circulating estrogen would enable the regulatory response to apo- and holo-Tf infusions that were seen in males. We found that reducing peripheral estrogen did not change the lack of response of ^{55}Fe-Tf uptake into MVs and release into the brain following infusion of apo- or holo-Tf. However, the variability that had been seen in the intact females was significantly reduced to that seen in males after removal of circulating estrogen. Additionally, delivery of Fth1 bound iron was not responsive to the ratio of apo- to holo-Tf in the CSF of either males or females. A particularly notable finding in this study was that MVs contained significantly more of the injected iron regardless of the delivery protein than the brain parenchyma even though the MVs account for only 2% of the total brain cells[10]. This finding further establishes our position that the ECs serve as a reservoir for iron for subsequent regulated release into the brain. Previous studies reporting on uptake of iron or other nutrients have rarely differentiated what is in the microvasculature versus what has entered the brain parenchyma. Furthermore, our data demonstrate that acquisition of brain iron is dependent on carrier protein and sex.

Previously, we and other have postulated the concept of regulation of iron release to the brain by endothelial cells of the BBB in cell culture models[13–16, 24,25]. For example, Simpson *et al.* demonstrated that CSF from iron deficient monkeys, as well as conditioned media from iron chelated astrocytes, increased iron release from bovine retinal endothelial cells[16] in a bi-chamber model of the BBB. Moreover, our group previously showed, using iPSC-derived ECs in a simulated BBB model, that exposure to apo-Tf resulted in increases in both ^{59}Fe-Tf and ^{59}Fe-Fth1 transport from apical to basal chambers, whereas incubation with holo-Tf decreased their transport[14]. *In vitro* conditions simulating iron deficient environments have repeatedly resulted in increased iron transport across the BBB[16,26,27]. However, until now, the demonstration of *in vivo* regulation was lacking. Our *in vivo* data from male mice support regulated release of iron from ECs forming the MV and suggest that the brain uses apo- and holo-Tf to relay its iron status to ECs, which in turn release more or less iron in response. An example of how this feedback can occur *in situ* is that, following iron uptake by neurons and astrocytes, these cells release apo-Tf into the extracellular fluid[28,29]. Thus, areas of greater energetic activity can regionally signal for increased iron release from MVs. Thus, our data address for the first time local regulation of brain iron

uptake in response to iron utilization and help explain the findings of Beard *et al.* who demonstrated that brain iron uptake differs in various regions[30].

The role of Fth1 as an iron delivery protein to the brain is a relatively new concept with great implications as it binds nearly 2000 times more iron than Tf[31]. It has been reported that Fth1 can replace Tf as the iron delivery protein for oligodendrocytes[32] and ECs[14]. Fth1 is a substantial iron contributor to the brain during development, as up to postnatal day 22, mice take up significantly more Fth1 bound iron than Tf bound iron into the brain[18]. In previous *in vitro* studies, the iron status of Tf in the basal compartment of the BBB model impacted the amount of Fth1-bound iron that was transported across the ECs[14]. However, in this *in vivo* study, we did not see any significant differences in Fth1 bound iron uptake into MVs or release into the brain following infusion of apo- or holo-Tf. In females, the infusion of apo-Tf did result in a two-fold increase in iron release into the brain compared to sham control. Although this difference did not reach statistical significance, the Cohen's *d* effect size between sham control and apo-Tf is 0.65, indicating a moderate effect. The absence of statistical significance was likely due to the variability in the different groups. Thus, the data suggest that Fth1 delivered iron is responsive to CSF iron deficiency in females.

In a few experiments conducted, infusion of aCSF increased iron uptake into MVs and release into the brain. Based on our calculations, the 0.25 µl/hour infusion rate would have resulted in an approximately 1% dilution of total CSF and, thus, should have minimal effect on endogenous Tf signals with complete turnover every 1.8 hours in the mouse[33]. It is possible that in the less than 1 µl volume of the mouse lateral ventricle[34] this initial dilution is locally greater and results in a more regional iron uptake and release. Regardless, the observation that apo-Tf or aCSF increases the uptake of transferrin-bound iron to the brain and release by the microvasculature underscores how exquisitely fined tuned the signaling from the brain to the MVs regarding iron status is.

Significant sex differences were detected in baseline (sham control group) iron uptake between Tf and Fth1. Female mice took up significantly more iron bound to Tf than to Fth1, while there was no statistically significant difference in iron uptake by either delivery protein in males. There was an increased proportion of Tf-bound iron released into the brain in females relative to males, indicating that iron was more rapidly released to the brain. The differences in baseline uptake would suggest differences in iron levels in the brain but studies have shown there is little to no difference in total brain iron levels between males and females[35,36]. These studies, however, largely fail to examine the process of iron accumulation. Brain iron accumulation was addressed by Duck *et al.*, who showed that 24 hours after injecting mice with ^{59}Fe-Tf, males and females had the same amount of iron uptake; however, after five days post injection, females took up significantly more ^{59}Fe than males[20]. Combined with our data presented herein, these findings indicates that females have more iron uptake over time than males. More iron accumulation by females compared to males would be consistent with increased in myelin turnover[37] and dopamine synthesis[38,39] reported in females; both processes are dependent on iron as a co-factor[40,41]. The constant utilization of iron for these metabolic processes likely leads to an increased

requirement of iron uptake into the brain which seems to be predominantly met by regulation of Fth1. This idea is also consistent with the lack of Tf delivered iron response by females to the infusion of apo- and holo-Tf. Future studies to decipher how differences in metabolic needs impact female brain iron uptake are needed.

In conclusion, this study is the first demonstration of *in vivo* regulation of brain iron uptake into MVs and subsequent release into the brain by apo- and holo-Tf. Moreover, we have identified striking sex differences in the baseline uptake and regulation of iron uptake for both Tf and Fth1. Understanding the sex differences and differences in Tf versus Fth1 delivered iron is crucial for clinical translation of these studies for the treatment of brain iron dysregulation and use for drug delivery efforts.

Abbreviations

- Blood-brain barrier (BBB)
- Endothelial cells (ECs)
- Transferrin (Tf)
- Ferritin heavy chain (Fth1)
- Artificial cerebrospinal fluid (aCSF)
- Microvessels (MVs)
- Ovariectomy (OVX)

Declarations

Funding:

Funding for this study was provided by NIH R01NS113912-01 (JRC) and NIH TL1TR002014 (SLB).

Acknowledgments:

The authors would like to thank Quinn Wade for technical assistance, Dr. Todd Schell for use of the Hidex 300 SL (LabLogic), and the Health Physics Department at Penn State College of Medicine for radioisotope assistance.

Author Contributions:

SLB and EBN performed animal experiments. SLB performed additional protein analyses. KP performed TIBC analysis. SLB, IAS, and JRC designed research. All authors analyzed data, edited, and contributed to writing the paper.

Disclosure/Conflict of Interest:

JRC is the founder and chairman of the board of Sidero Biosciences LLC, a company with a product involving oral delivery of ferritin for management of iron deficiency.

References

1. Dev S, Babitt JL. Overview of Iron Metabolism in Health and Disease. Hemodial Int 2017; 21: S6–S20.
2. Connor JR, Boyer PJ, Menzies SL, et al. Neuropathological examination suggests impaired brain iron acquisition in restless legs syndrome. Neurology 2003; 61: 304–309.
3. O'Keeffe ST, Gavin K, Lavan JN. Iron status and restless legs syndrome in the elderly. Age Ageing 1994; 23: 200–203.
4. Earley CJ, B Barker P, Horská A, et al. MRI-determined regional brain iron concentrations in early- and late-onset restless legs syndrome. Sleep Med 2006; 7: 458–461.
5. Kim Y, Connor JR. The roles of iron and HFE genotype in neurological diseases. Mol Aspects Med 2020; 75: 100867.
6. Wang J-Y, Zhuang Q-Q, Zhu L-B, et al. Meta-analysis of brain iron levels of Parkinson's disease patients determined by postmortem and MRI measurements. Sci Rep 2016; 6: 36669.
7. Gajowiak A, Styś A, Starzyński RR, et al. Misregulation of iron homeostasis in amyotrophic lateral sclerosis. Postepy Hig Med Dosw (Online) 2016; 70: 709–721.
8. Ayton S, Wang Y, Diouf I, et al. Brain iron is associated with accelerated cognitive decline in people with Alzheimer pathology. Molecular Psychiatry 2019; 1–10.
9. Liu J-L, Fan Y-G, Yang Z-S, et al. Iron and Alzheimer's Disease: From Pathogenesis to Therapeutic Implications. Front Neurosci 2018; 12: 632.
10. Goldstein GW, Betz AL. The blood-brain barrier. Sci Am 1986; 255: 74–83.
11. McCarthy RC, Kosman DJ. Iron transport across the blood-brain barrier: development, neurovascular regulation and cerebral amyloid angiopathy. Cell Mol Life Sci 2015; 72: 709–727.
12. Taylor EM, Morgan EH. Developmental changes in transferrin and iron uptake by the brain in the rat. Brain Res Dev Brain Res 1990; 55: 35–42.
13. McCarthy RC, Kosman DJ. Mechanisms and regulation of iron trafficking across the capillary endothelial cells of the blood-brain barrier. Front Mol Neurosci 2015; 8: 31.
14. Chiou B, Neal EH, Bowman AB, et al. Endothelial cells are critical regulators of iron transport in a model of the human blood-brain barrier. J Cereb Blood Flow Metab 2019; 39: 2117–2131.
15. Duck KA, Simpson IA, Connor JR. Regulatory mechanisms for iron transport across the blood-brain barrier. Biochem Biophys Res Commun 2017; 494: 70–75.
16. Simpson IA, Ponnuru P, Klinger ME, et al. A novel model for brain iron uptake: introducing the concept of regulation. J Cereb Blood Flow Metab 2015; 35: 48–57.

17. Fisher J, Devraj K, Ingram J, et al. Ferritin: a novel mechanism for delivery of iron to the brain and other organs. Am J Physiol Cell Physiol 2007; 293: C641-649.
18. Chiou B, Neely EB, Mcdevitt DS, et al. Transferrin and H-ferritin involvement in brain iron acquisition during postnatal development: impact of sex and genotype. Journal of Neurochemistry 2020; 152: 381–396.
19. Fiandra L, Mazzucchelli S, Truffi M, et al. In Vitro Permeation of FITC-loaded Ferritins Across a Rat Blood-brain Barrier: a Model to Study the Delivery of Nanoformulated Molecules. *J Vis Exp*. Epub ahead of print 22 August 2016. DOI: 10.3791/54279.
20. Duck KA, Neely EB, Simpson IA, et al. A role for sex and a common HFE gene variant in brain iron uptake. J Cereb Blood Flow Metab 2018; 38: 540–548.
21. Wade QW, Chiou B, Connor JR. Iron uptake at the blood-brain barrier is influenced by sex and genotype. Adv Pharmacol 2019; 84: 123–145.
22. Hladky SB, Barrand MA. Mechanisms of fluid movement into, through and out of the brain: evaluation of the evidence. Fluids Barriers CNS 2014; 11: 26.
23. Aldred AR, Dickson PW, Marley PD, et al. Distribution of transferrin synthesis in brain and other tissues in the rat. J Biol Chem 1987; 262: 5293–5297.
24. Burdo JR, Antonetti DA, Wolpert EB, et al. Mechanisms and regulation of transferrin and iron transport in a model blood-brain barrier system. Neuroscience 2003; 121: 883–890.
25. Moos T. Brain iron homeostasis. Dan Med Bull 2002; 49: 279–301.
26. Siddappa AJM, Rao RB, Wobken JD, et al. Iron Deficiency Alters Iron Regulatory Protein and Iron Transport Protein Expression in the Perinatal Rat Brain. Pediatr Res 2003; 53: 800–807.
27. Connor JR, Duck K, Patton S, et al. Evidence for communication of peripheral iron status to cerebrospinal fluid: clinical implications for therapeutic strategy. Fluids Barriers CNS 2020; 17: 28.
28. Moos T, Morgan EH. The metabolism of neuronal iron and its pathogenic role in neurological disease: review. Ann N Y Acad Sci 2004; 1012: 14–26.
29. Ji C, Kosman DJ. Molecular mechanisms of non-transferrin-bound and transferring-bound iron uptake in primary hippocampal neurons. J Neurochem 2015; 133: 668–683.
30. Beard JL, Wiesinger JA, Li N, et al. Brain iron uptake in hypotransferrinemic mice: influence of systemic iron status. J Neurosci Res 2005; 79: 254–261.
31. Harrison PM, Arosio P. The ferritins: molecular properties, iron storage function and cellular regulation. Biochim Biophys Acta 1996; 1275: 161–203.
32. Chiou B, Lucassen E, Sather M, et al. Semaphorin4A and H-ferritin utilize Tim-1 on human oligodendrocytes: A novel neuro-immune axis. Glia 2018; 66: 1317–1330.
33. Pardridge WM. CSF, blood-brain barrier, and brain drug delivery. Expert Opin Drug Deliv 2016; 13: 963–975.
34. Hino K, Otsuka S, Ichii O, et al. Strain differences of cerebral ventricles in mice: can the MRL/MpJ mouse be a model for hydrocephalus? Jpn J Vet Res 2009; 57: 3–11.

35. Uchino E, Tsuzuki T, Inoue K. The effects of age and sex on seven elements of Sprague-Dawley rat organs. Lab Anim 1990; 24: 253–264.
36. Hahn P, Song Y, Ying G, et al. Age-dependent and gender-specific changes in mouse tissue iron by strain. Experimental Gerontology 2009; 44: 594–600.
37. Cerghet M, Skoff RP, Bessert D, et al. Proliferation and death of oligodendrocytes and myelin proteins are differentially regulated in male and female rodents. J Neurosci 2006; 26: 1439–1447.
38. McDermott JL, Liu B, Dluzent DE. Sex Differences and Effects of Estrogen on Dopamine and DOPAC Release from the Striatum of Male and Female CD-1 Mice. Experimental Neurology 1994; 125: 306–311.
39. Munro CA, McCaul ME, Wong DF, et al. Sex Differences in Striatal Dopamine Release in Healthy Adults. Biological Psychiatry 2006; 59: 966–974.
40. Cheli VT, Correale J, Paez PM, et al. Iron Metabolism in Oligodendrocytes and Astrocytes, Implications for Myelination and Remyelination. ASN Neuro 2020; 12: 1759091420962681.
41. Khan FH. Iron, dopamine, genetics, and hormones in the pathophysiology of restless legs syndrome. J Neurol 2017; 8.

Figures

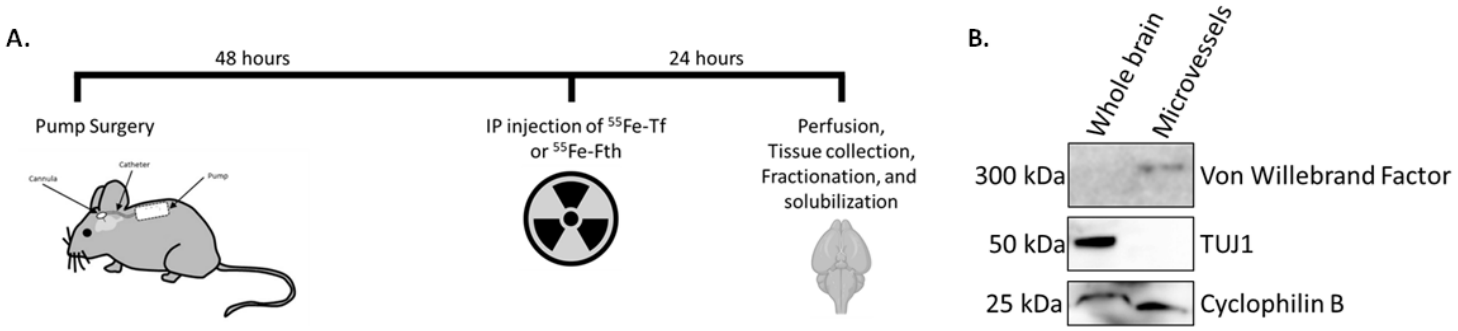

Figure 1

Experimental setup. Mini osmotic pumps were inserted subcutaneously in three-month-old male and female mice (**A**). Pumps contained nothing (sham), aCSF, 1 mg/ml apo-Tf, or 1 mg/ml holo-Tf. Forty-eight hours after the surgery, mice were injected IP with radioactive ^{55}Fe-Tf or ^{55}Fe-Fth1. Twenty-four hours later the mice were euthanized and perused. Brains were collected and homogenized. Microvessels (MV) were isolated from the whole brain using centrifugation. Both fractions of MVs and whole brain were further solubilized. Radioactivity in each fraction was determined using liquid scintillation counting. Western blotting was performed on whole brain and MV fractions (**B**). The blots show von Willebrand factor, an endothelial cell specific marker, present in the MV fraction and not in the whole brain fraction. TUJ1, a neuronal marker, is shown in the whole brain fraction and not the MV fraction. Cyclophilin B was used as a loading control for samples.

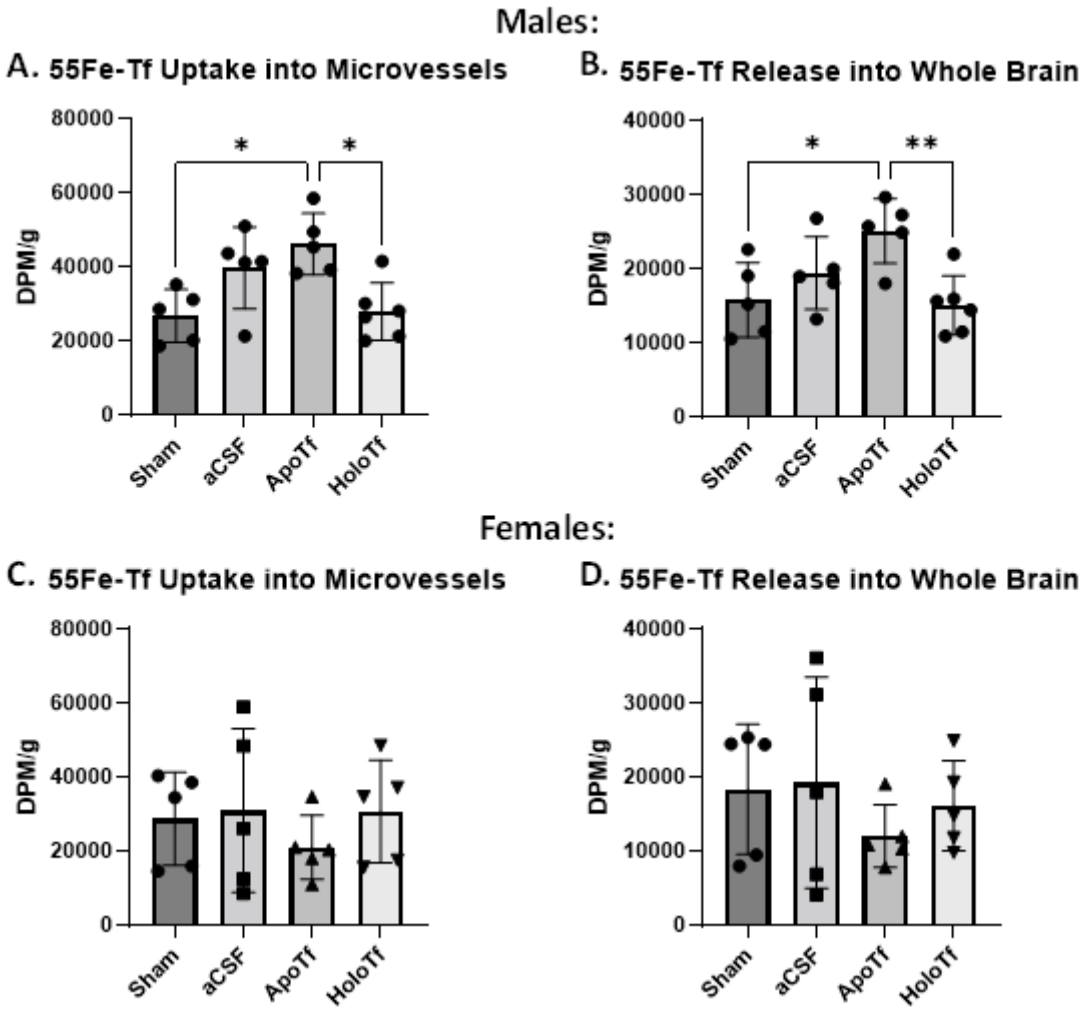

Figure 2

^{55}Fe-Tf brain uptake in males and females. Samples are reported as DPM per gram of brain tissue. In males, increasing levels of apo-Tf in the brain significantly increases ^{55}Fe-Tf uptake into MVs (**A**) and release into the brain (**B**). Additionally, increasing levels of holo-Tf results in significantly reduced ^{55}Fe-Tf uptake compared to infusions of apo-Tf. However, in females, the ratio of apo- to holo-Tf in the brain has little regulatory effect on ^{55}Fe-Tf uptake into MVs (**C**) and release into the brain (**D**). n= 5 for all conditions, means of biological replicates ± SD were evaluated for statistical significance using one-way ANOVA with Tukey's posttest for significance. * $p<0.05$, ** $p<0.01$

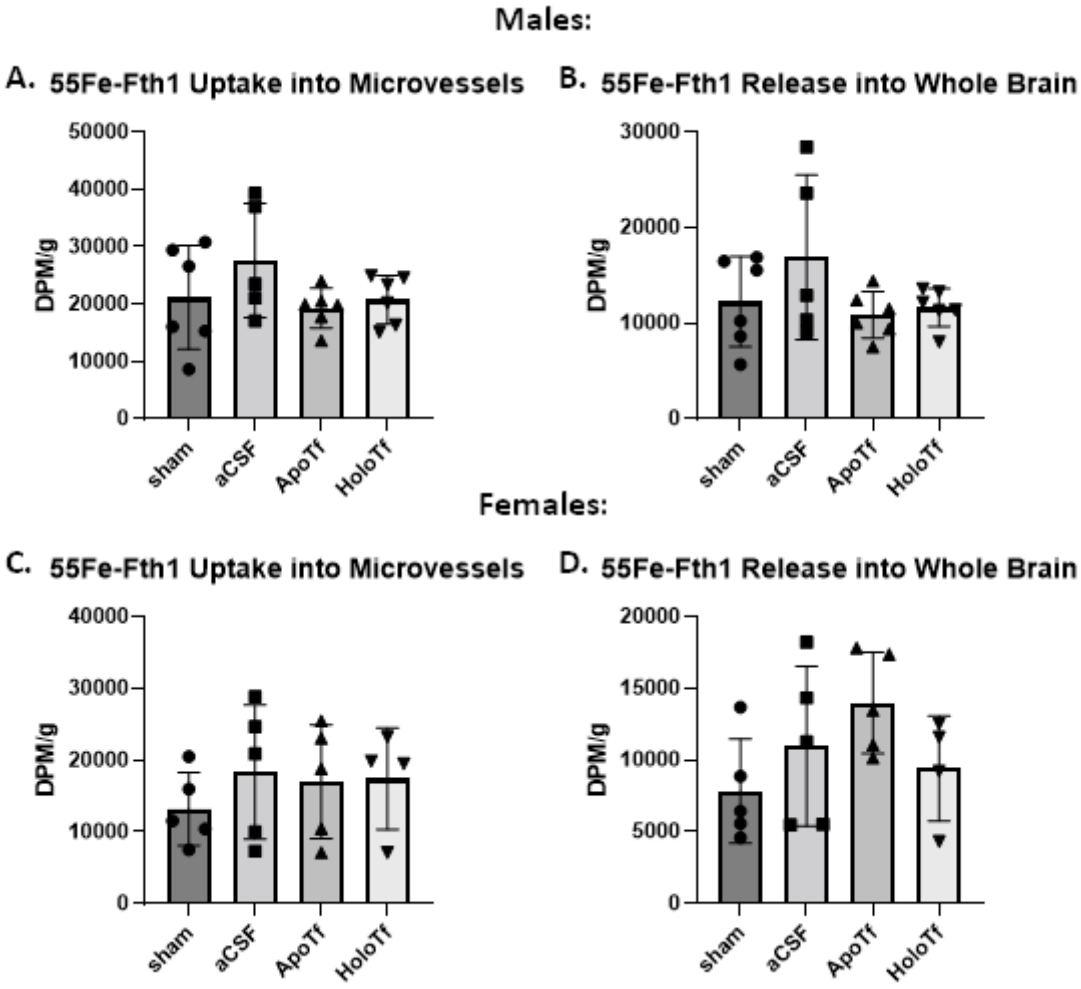

Figure 3

^{55}Fe-Fth1 brain uptake in males and females. Samples are reported as DPM per gram of brain tissue. In males, the ratio of apo- to holo-Tf in the brain has little regulatory effect on uptake into MVs (**A**) and release into the brain (**B**). In females, the ratio of apo- to holo-Tf in the brain has little regulatory effect on uptake into MVs (**C**) but increased ratio of apo-Tf increases release into the brain (**D**). Notably, the MVs contain substantially more ^{55}Fe than the entirety of the brain, supporting the role of MVs in regulating iron release. n= 5 to 6 for all conditions, means of biological replicates ± SD were evaluated for statistical significance using one-way ANOVA with Tukey's posttest for significance.

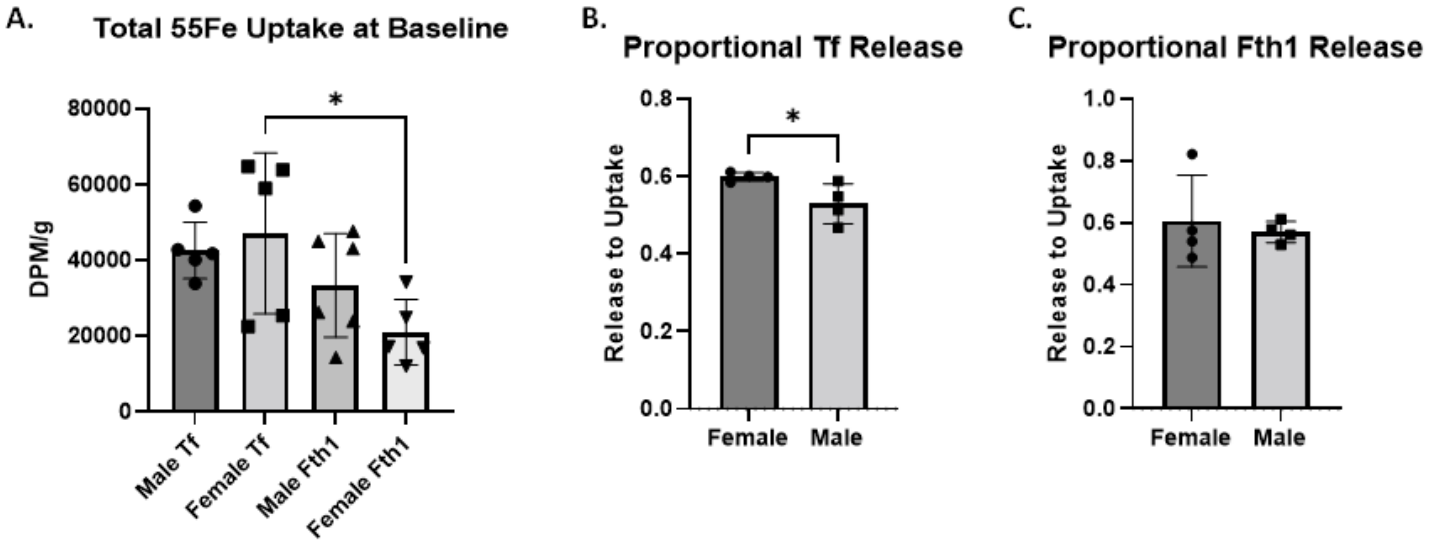

Figure 4

Differences in baseline iron uptake. When pooling the ^{55}Fe present in both MV and whole brain fractions (**A**), females take up significantly more ^{55}Fe when bound to Tf than Fth1. Of note, the variability of ^{55}Fe-Tf uptake and release in females is substantial. The coefficient of variability of the sham condition in females is 45.09%. The corresponding coefficient of variability of this condition in males is 17.43%. When further exploring the proportion of ^{55}Fe-Tf that is released into the brain to the amount that is taken up into the MVs, females release significantly more of the iron the MVs take up compared to males (**B**). There was no difference between males and females on the proportion of ^{55}Fe-Fth1 release to uptake (**C**). n= 5 to 6 for all conditions, means of biological replicates ± SD were evaluated for statistical significance using one-way ANOVA with Tukey's posttest for significance for A. Proportions of release to uptake for each infusion condition were calculated and plotted, means ± SD were evaluated for statistical significance using unpaired t-test for significance for B and C. * $p<0.05$

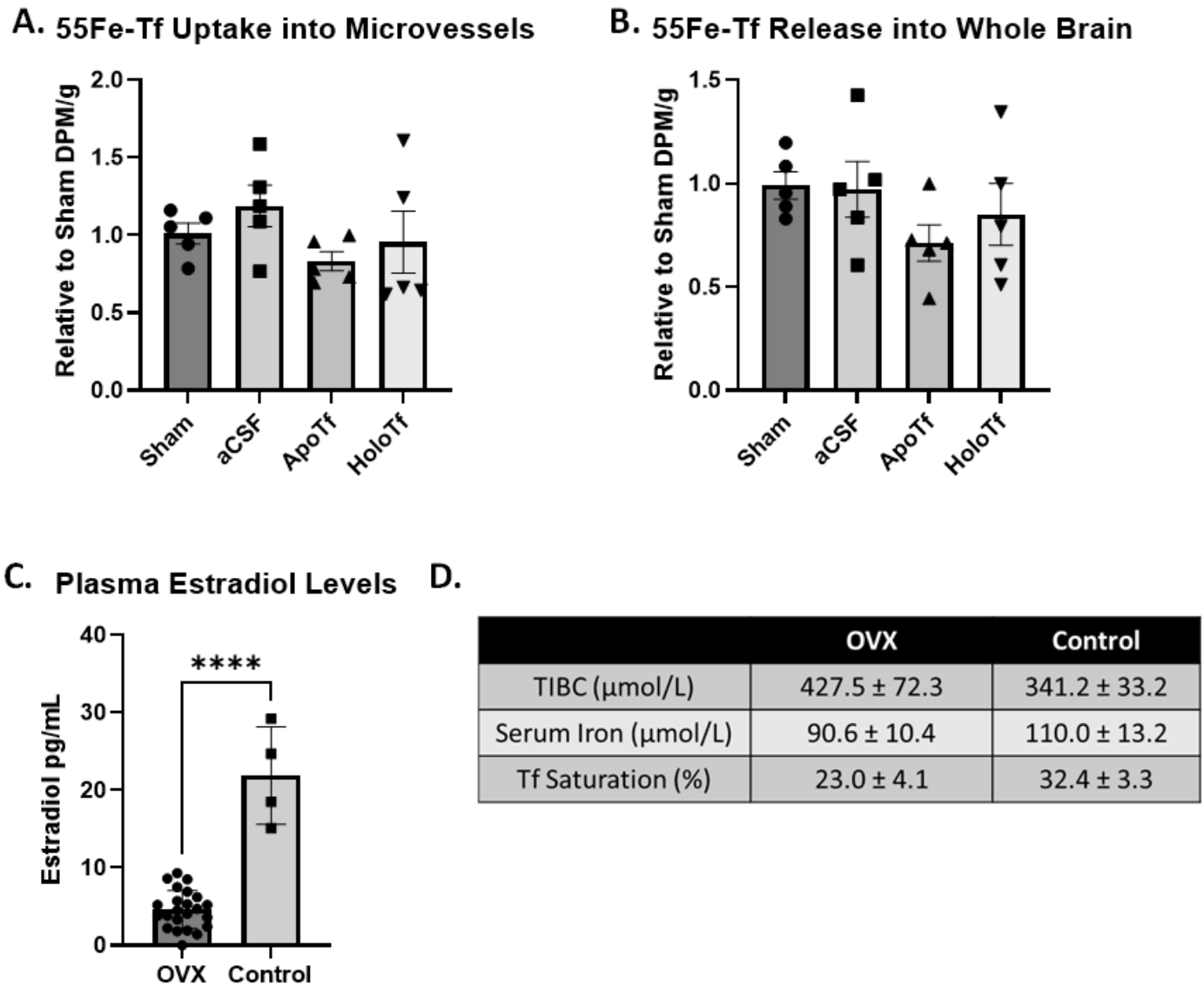

D.

	OVX	Control
TIBC (µmol/L)	427.5 ± 72.3	341.2 ± 33.2
Serum Iron (µmol/L)	90.6 ± 10.4	110.0 ± 13.2
Tf Saturation (%)	23.0 ± 4.1	32.4 ± 3.3

Figure 5

OVX on ^{55}Fe-Tf brain uptake in females. Samples are reported as DPM per gram of brain tissue. After removing circulating estrogen via OVX, female mice still do not show increased ^{55}Fe-Tf uptake (**A**) or release (**B**) across infusion conditions relative to sham. The coefficient of variability of ^{55}Fe-Tf uptake in sham conditions was 16.15%. The levels of plasma estradiol levels were determined to confirm the success of the OVX in all mice used (**C**). The TIBC of plasma is higher in OVX mice while the Tf saturation percentage and serum iron are lower when compared to control. (**D**). n= 5 for all conditions, means of biological replicates ± SD were evaluated for statistical significance using one-way ANOVA with Tukey's posttest for significance for A and B. Means ± SD were evaluated for statistical significance using unpaired t-test for significance for C and D. **** $p<0.0001$